Malik, N. A., Anantharamaiah, G. M., Gawish, A., & Cheung, H. C. (1987) *Biochim. Biophys. Acta 911*, 221–230.
Marchiori, F., Borin, G., Chessa, G., Cavaggion, G., Michelin, L., & Peggion, E. (1983) *Hoppe-Seyler's Z. Physiol. Chem. 364*, 1019–1028.
Marsden, B. J., Hodges, R. S., & Sykes, B. D. (1988) *Biochemistry 27*, 4198–4206.
Millero, F. J. (1971) *Chem. Rev. 71*, 147–176.
Millero, F. J. (1972) in *Water and Aqueous Solutions* (Horne, R. A., Ed.) pp 519–595, Wiley-Interscience, New York.
Pavone, V., DiNola, A., Andini, S., Ferrara, L., DiBlasio, D., Benedetti, E., & Pucci, P. (1984) *Int. J. Pept. Protein Res. 23*, 454–461.
Rashin, A. A., & Honig, B. (1985) *J. Phys. Chem. 89*, 5588–5593.
Rebek, J., Jr. (1987) *Science 235*, 1478–1484.
Reid, R. E. (1987) *Biochemistry 26*, 6070–6073.
Reid, R. E., & Hodges, R. S. (1980) *J. Theor. Biol. 84*, 401–444.
Reid, R. E., Clare, D. M., & Hodges, R. S. (1980) *J. Biol. Chem. 255*, 3642–3646.
Reid, R. E., Gariépy, J., Saund, A. K., & Hodges, R. S. (1981) *J. Biol. Chem. 256*, 2742–2751.
Roberts, D. M., Lukas, T. J., & Watterson, D. M. (1986) *CRC Crit. Rev. Plant Sci. 4*, 311–339.
Satyshur, K. A., Rao, S. T., Pyzalska, D., Drendel, W., Greaser, M., & Sundaralingam, M. (1988) *J. Biol. Chem. 263*, 1628–1647.
Schauer, C. K., & Anderson, O. P. (1987) *J. Am. Chem. Soc. 109*, 3646–3656.
Schauer, C. K., & Anderson, O. P. (1989) *J. Chem. Soc., Dalton Trans.*, 185–191.
Shannon, R. D. (1976) *Acta Crystallogr., Sect. A 32*, 751–767.
Stewart, J. M., & Young, J. D. (1984) in *Solid Phase Peptide Synthesis*, Pierce Chemical Co., Rockford, IL.
Szebenyi, D. M. E., & Moffat, K. (1986) *J. Biol. Chem. 261*, 8761–8777.
Toda, A., Yazawa, M., Kondo, K., Honma, T., Narita, K., & Yagi, K. (1981) *J. Biochem. (Tokyo) 90*, 1493–1505.
Virender, K. S., Kent, S. B. H., Tam, J. P., & Merrifield, R. B. (1981) *Anal. Biochem. 117*, 147–157.
Yokote, Y., Murayama, A., & Akahane, K. (1986) *Anal. Biochem. 152*, 245–249.

Use of Site-Directed Mutagenesis To Destabilize Native Apomyoglobin Relative to Folding Intermediates†

Frederick M. Hughson and Robert L. Baldwin*
Department of Biochemistry, Stanford University Medical Center, Stanford, California 94305
Received November 15, 1988; Revised Manuscript Received February 6, 1989

ABSTRACT: Site-directed mutagenesis has been used to study the effect on the stability of human apomyoglobin (apoMb) of modifying the size, hydrophobicity, and charge of a central residue in the G·B helix–helix packing interface. Some stability measurements have also been made on the corresponding holomyoglobins (heme present). Cys-110, a central helix pairing residue in the G helix, has been changed to Ala, Ser, Asp, and Leu. Stability to low-pH-induced unfolding has been measured for both native apoMb and the compact folding intermediate discovered by Griko et al. [Griko, Y. V., Privalov, P. L., Venyaminov, S. Y., & Kutyshenko, V. P. (1988) *J. Mol. Biol. 202*, 127–138]. As judged by its circular dichroism spectrum, this intermediate has a substantial helix content (about 35%). Whether or not this inferred helical structure is closely related to the myoglobin structure is not yet known. The mutational evidence shows that integrity of G·B helix pairing is important for the stability of apoMb as well as of myoglobin and that this helix pairing site is very sensitive to both steric and electrostatic disruption. Our results also suggest that G·B helix pairing does not stabilize the compact intermediate; hence, disrupting this site destabilizes the native protein relative to the compact intermediate. Such selective destabilization of the native state relative to equilibrium folding intermediates is not restricted to acid denaturation: urea denaturation of the Leu mutant appears to display at least one stable intermediate, while wild-type and the remaining mutant apoMbs undergo two-state urea unfolding transitions.

Apomyoglobin (apoMb)[1] is the classic example of a protein whose folding pathway has been inferred from its structure. In particular, the framework model of folding is based in part on the postulated folding behavior of apoMb (Ptitsyn & Rashin, 1975; Richmond & Richards, 1978; Cohen et al., 1979), in which individual α-helices form independently of each other but are stabilized by helix pairing reactions, so that a stable framework of helical structure is formed which acts as a hydrophobic container for the heme group. Recently, Griko et al. (1988) have shown, especially by calorimetric measurements, that apoMb has a well-organized hydrophobic core and may be considered as a well-defined globular protein. In view of its significance for the framework model of folding,

† This work was supported by NIH Grant GM 19988.

[1] Abbreviations: apoMb, apomyoglobin; CD, circular dichroism; GuHCl, guanidine hydrochloride; HEPES, *N*-(2-hydroxyethyl)-piperazine-*N*′-2-ethanesulfonic acid; Mb, myoglobin; N, I, and U, native, acid intermediate, and unfolded states of apomyoglobin, respectively.

0006-2960/89/0428-4415$01.50/0

it is tempting to investigate the folding pathway of apoMb. This is particularly true since Griko et al. (1988) have found that acid unfolding of apoMb reveals a compact folding intermediate, whose properties seem similar to the "molten globule intermediates" reviewed recently by Ptitsyn (1987). We begin such a study here by using site-directed mutagenesis to ask if a particular helix pairing reaction, between the B and G helices, is important for the stability of apoMb and of the compact intermediate.

ApoMb, myoglobin (Mb) without the heme group, is a small (molecular weight 17000) monomeric protein with no disulfide bonds. Approximately 60% α-helix, the apoprotein has about 20 fewer residues in a helical conformation than the holoprotein (Harrison & Blout, 1965). ^{1}H NMR and calorimetric evidence (Griko et al., 1988) indicate that sperm whale apoMb has a unique three-dimensional structure which, although unknown, presumably resembles that of Mb. ApoMb is most stable at 27 °C; either raising or lowering the temperature destabilizes the native state (Griko et al., 1988). In their thorough study of sperm whale apoMb stability, Griko et al. monitored α-helix content as a function of pH. As the pH is lowered from 6 to 2 in low-salt buffer, apoMb unfolds, and its α-helix content drops from ~60% to <15%. At 27 °C, acid denaturation occurs as a single, cooperative transition. Surprisingly, however, at both low (−6 °C) and high (50 °C) temperatures, acid denaturation reveals two successive unfolding transitions well separated by a plateau region (Griko et al., 1988). This plateau represents a partially folded equilibrium intermediate. Whether this intermediate is on the direct folding pathway is not yet known. The α-helix content of the intermediate is approximately 35%, midway between that of the native (N) and unfolded (U) protein. The appearance of an intermediate at both high and low temperatures is most likely caused by the onset of heat and cold denaturation, respectively: both processes destabilize the N state more than they destabilize the acid intermediate (I). Irace and co-workers have also observed apoMb intermediates under some conditions (Balestrieri et al., 1976; Irace et al., 1981, 1986; Colonna et al., 1982).

The I state of apoMb is compact (Griko et al., 1988) and thus resembles the "molten globule" state discussed by Ohgushi and Wada (1983) and reviewed by Ptitsyn (1987). Several proteins have been shown to form compact intermediates under specified conditions. The best-characterized example is the A state of α-lactalbumin, observed both at low pH and at intermediate GuHCl concentrations, which is nearly as compact as the native protein (Kuwajima et al., 1976; Dolgikh et al., 1985). The secondary structure of the A state, as judged by circular dichroism (CD), also resembles that of native α-lactalbumin. Tertiary interactions present in the native protein are not observed in the A state (Kuwajima et al., 1976; Dolgikh et al., 1985). Ikeguchi et al. (1986b) have shown that this equilibrium intermediate has properties indistinguishable from an early intermediate in the kinetic folding pathway.

We have targeted a specific tertiary interaction in apoMb for site-directed mutagenesis: the G·B helix–helix pairing site. We assume, on the basis of the close similarity among the known globin structures, that the three-dimensional structures of human and sperm whale Mbs are very similar; their primary sequences differ at 25 of 153 positions, of which many are conservative substitutions. Thus, we use the crystal structure of sperm whale Mb (Takano, 1977) to select residue 110 of human Mb for site-directed mutagenesis. Residue 110 is positioned near the middle of the G helix, and its side chain is buried almost entirely in the G·B helix packing interface

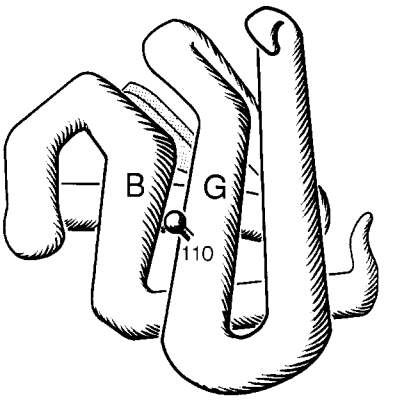

FIGURE 1: Schematic representation of Mb, showing the relative orientation of the B and G helices. The heme group is shown as a shaded disk. The β-carbon position of residue 110 is also indicated schematically.

(Figure 1). We have made a series of substitutions varying the size, hydrophobicity, and charge of this central buried residue. We test whether the overall architecture of apoMb resembles that of Mb closely enough that mutations predicted to disrupt a helix pairing site in Mb also destabilize native apoMb. Because the acid denaturation of apoMb at low temperature occurs in two well-separated stages, the effect of mutations on the stability of the N and I states can be assessed independently. In this way, we are able to investigate the role of a particular tertiary interaction in stabilizing the native protein and/or the compact acid intermediate.

Experimental Procedures

Preparation of Mutant Mbs and ApoMbs. Two methods were used to create site-directed mutations at position 110 of human Mb. The vector M13mp11FXMb (Varadarajan et al., 1985) was primed with synthetic oligonucleotides to substitute the codons TCC (Ser), CTC (Leu), and GAC (Asp) for the wild-type codon TGC (Cys). The Ser and Leu mutants were made by using a 10-fold excess of mutagenic oligonucleotide to prime second-strand synthesis by the large fragment of DNA polymerase I. The extension reaction was transformed directly into *Escherichia coli* strain TG1. The resulting phage plaques were then transferred to nitrocellulose and probed with labeled oligonucleotide under stringent conditions to identify mutants. The Asp mutant was made by using the method of Kunkel et al. (1987). In all cases, the entire coding region was sequenced (Sanger, 1981) to confirm that only the expected changes had been made and then subcloned into pLcIIFXβ (Nagai & Thogersen, 1984) to express the mutant Mbs. The resulting plasmids, upon transformation into *E. coli* strain MZ1, direct high-level synthesis of fusion proteins in which the first 31 amino acids of λ cII protein are fused via the sequence Gly-Gly-Ser-Ile-Glu-Gly-Arg to the amino terminus of Mb. Identical expression constructs pMb3 [carrying the wild-type human Mb gene (Varadarajan et al., 1985)] and pMb3[C110A] [as pMb3, but coding for the mutant human Mb Cys-110 → Ala (Varadarajan, 1988)] were the gift of R. Varadarajan. Overexpression, reconstitution with heme, and trypsin cleavage of the fusion protein, as well as purification of the resultant wild-type and mutant Mbs, were performed as described by Varadarajan et al. (1989). All purified Mbs were >95% homogeneous as judged by sodium dodecyl sulfate–polyacrylamide gel electrophoresis and had essentially identical absorbance spectra at 250–700 nm.

ApoMbs were prepared from Mbs by using a minor modification of the 2-butanone extraction method of Teale (1959): following extraction of the heme group, the protein solution

was dialyzed extensively against 1 mM HCl at 4 °C. For wild-type apoMb, the dialysis buffer also contained 1 mM dithiothreitol to prevent formation of covalent dimers involving Cys-110. Prepared in this way, apoMbs were stable for up to 1 week at 4 °C.

ApoMb concentration was determined by measuring the UV absorbance in 6 M GuHCl/20 mM sodium phosphate, pH 6.5, and using extinction coefficients derived from the tryptophan and tyrosine content as determined by Edelhoch (1967). This procedure yields extinction coefficients for horse apoMb and several other proteins which agree closely with those determined by other means (Edelhoch, 1967). Calculated in this way, ϵ_{280} and ϵ_{288} for the human apoMbs are 13.9 and 10.4 mM^{-1} cm^{-1}, respectively. Mb concentrations were determined by measuring the absorbance at 409 nm in 100 mM sodium phosphate, pH 6.8, and using an extinction coefficient of 171 mM^{-1} cm^{-1} (Puett, 1973).

Acid Denaturation. Acid denaturation curves were generated by measuring the CD signal at 222 nm, $[\theta]_{222}$, as a function of pH using an Aviv 60DS spectropolarimeter. Two hundred microliters of apoMb stock (5.00 μM protein in 1 mM HCl) was added to 1.80 mL of buffer solution on ice to give final conditions of 500 nM apoMb, 5 mM NaCl, 1 mM sodium phosphate, and 1 mM sodium citrate. The pH of the buffer solution was adjusted beforehand with HCl. For wild-type apoMb, 1 mM dithiothreitol was included in both protein stock and buffer solutions. Since Cys-110 is the sole cysteine in human apoMb, dithiothreitol was omitted from solutions containing position 110 mutants. In a control experiment, dithiothreitol had no effect on the transition curves for acid or urea denaturation of the Ala mutant. CD measurements were made in a 10-mm quartz cuvette thermostated to 3.0 ± 0.5 °C. At this protein concentration (500 nM), little or no time-dependent change in the CD signal was observed, while at higher concentrations time-dependent changes in the signal were observed for the I state at some pH values. The rate of change of $[\theta]_{222}$ depended on apoMb concentration and was attributed to aggregation of the I state. pH was measured after allowing the samples to warm to room temperature at the conclusion of the experiment.

pH transition midpoints were estimated directly from inspection of plots of $[\theta]_{222}$ versus pH.

Urea and GuHCl Denaturation. Urea denaturation was monitored by measuring $[\theta]_{222}$ as a function of urea concentration at 3.0 ± 0.5 °C. Twenty microliters of apoMb stock (100 μM protein in 1 mM HCl) was added to 2.00 mL of ice-cold 10 mM *N*-(2-hydroxyethyl)piperazine-*N*′-2-ethanesulfonic acid (HEPES), pH 7.60, containing urea and, in the case of experiments with wild-type apoMb, 1 mM dithiothreitol. Values were obtained after an equilibration time of about 300 s. In the transition zone, slow irreversible changes in the CD signal were seen in both unfolding and refolding experiments and may reflect protein aggregation at moderate urea concentrations. Denaturation profiles, however, were independent of protein concentration between 1 and 5 μM apoMb.

Denaturation of the metMbs (the heme iron in the ferric state, water bound to the sixth coordination site) was monitored by measuring either $[\theta]_{222}$ or the Soret absorbance peak at 409 nm as a function of GuHCl concentration. The denaturant, GuHCl, and the conditions used were chosen to maximize the reversibility of the unfolding reaction; even so, reversibility was only 85–90%. Small volumes of Mb stock solution were added to GuHCl-containing 10 mM HEPES, pH 7.60, to give a final protein concentration of about 1 μM. The absorbance or CD signal was followed with time at 25.0 ± 0.1 °C. In the transition zone, both signals, after a rapid decrease, continued to decline gradually for several hours. This phenomenon generally has been attributed to heme or globin aggregation (Puett, 1973). "Apparent equilibrium" was defined as being reached when the rate of change of the signal reached 10% (of the native protein signal) per hour.

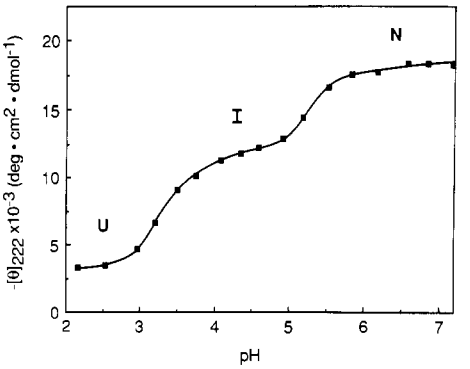

FIGURE 2: Acid denaturation of wild-type human apoMb. Mean residue ellipticity at 222 nm, $[\theta]_{222}$, is plotted as a function of pH. Protein concentration was 500 nM in 5 mM NaCl, 1 mM sodium phosphate, 1 mM sodium citrate, and 1 mM dithiothreitol. Sample temperature was 3 °C. Plateaus represent native (N), intermediate (I), and unfolded (U) states. The line through the data points was drawn by inspection.

Urea and GuHCl denaturation curves were analyzed by assuming that the folding/unfolding transition is two-state, in which case equilibrium constants (K_{app}) can be obtained at each denaturant concentration from the experimental data [specifically, $K_{app} = (y_N - y)/(y - y_D)$, where y represents the observable parameter ($[\theta]_{222}$ or ϵ_{409}) and y_N and y_D represent linear base lines for the native and denatured protein, respectively; Pace, 1986]. Since $\Delta G_{app} = -RT \ln K_{app}$, calculating the free energy of unfolding at a given denaturant concentration in the transition zone is straightforward. We assume that ΔG_{app} varies linearly with denaturant concentration (Schellman, 1978, 1987; Pace, 1986). Then $\ln K_{app}$ versus [denaturant] is also linear, and one can define a parameter $m = \mathrm{d} \ln K_{app}/\mathrm{d}[\text{denaturant}]$ which measures the cooperativity of the two-state transition (Shortle & Meeker, 1986). Six parameters then describe the denaturation curve: m, C_{mid} (the transition midpoint), and four parameters giving the slope and intercept of the two base lines (one each for native and unfolded protein). To derive values and standard deviations for these six parameters for a given data set, nonlinear least-squares analysis was performed using a program written by David Whitman and modified by Robert Fairman. To calculate $\Delta G°_{app}$, the apparent free energy of unfolding in the absence of denaturant, the formula $\Delta G°_{app} = RTmC_{mid}$ was used. This procedure is formally equivalent to extrapolating ΔG_{app} values derived from K_{app} in the transition zone back to 0 M denaturant, but it explicitly subjects the base lines, as well as the transition zone, to statistical treatment. An analogous treatment was published in greater detail recently (Santoro & Bolen, 1988). $\Delta\Delta G°_{app}$ is the change in $\Delta G°_{app}$ caused by a given mutation, using wild-type as the basis for comparison.

Results

Wild-type human apoMb unfolds in two well-separated cooperative transitions as the pH is lowered from 7 to 2 (Figure 2). The transition midpoints are pH 5.3 (N ↔ I) and pH 3.3 (I ↔ U) (Table I). ApoMbs from dog and horse (data not shown), as well as sperm whale (Griko et al., 1988), have very similar pH titration curves; a stable intermediate with

Table I: Transition pH Midpoints for Acid Denaturation of ApoMbs at 3 °C

apoMb	N ↔ I	I ↔ U
wild-type	5.3	3.3
C110A	5.1	3.5
C110S	5.2	3.7
C110D	5.9	3.7
C110L	6.2	3.2

an α-helix content of approximately 35% is seen in all cases. These four apoMbs share 80–90% amino acid sequence homology.

Four substitutions for Cys-110, a central residue in the G·B helix–helix packing site (Figure 1), were isolated by site-directed mutagenesis: Ala (C110A), Ser (C110S), Leu (C110L), and Asp (C110D). Acid denaturation curves for the mutant apoMbs (Figure 3) are reversible and still show the compact intermediate, although in some cases the pH midpoints of one or both transitions have shifted. At the low resolution afforded by CD measurements, residue 110 substitutions appear to alter the stability, but not the structure, of apoMb. The N states of the five apoMbs attain the same CD value within experimental error. $[\theta]_{222}$ values for the I and U states of all the apoMbs except C110L are also in reasonable agreement. Both I and U states of C110L appear to have, however, significantly higher $[\theta]_{222}$ values than wild-type apoMb or the remaining mutants. The structure of the I state may therefore be different, and residual structure in the U state may be augmented, for C110L relative to the remaining apoMbs. The I state appears to aggregate under some conditions (see Experimental Procedures); the use of low protein concentrations appears to circumvent this problem.

The pH midpoint for the transition from native to intermediate varies from pH 5.1 for C110A to pH 6.2 for C110L (see Table I), demonstrating that mutations at residue 110 affect the relative stability of N and I states. Compared to wild-type apoMb, the N states of C110D and C110L are significantly destabilized relative to the I states of these mutants, while the N states of C110A and C110S are marginally stabilized. It is therefore possible to vary the relative stability of N and I states of a protein over a broad range by engineering single amino acid changes.

Variation in the relative stabilities of the I and U states is less striking (Figure 3). The I state of the C110L mutant apoMb is the most stable, as it unfolds with the lowest pH midpoint of the apoMbs studied. The I states of C110S and C110D, and to a lesser extent C110A, are somewhat less stable than wild-type.

To characterize further the stability of the N states of the apoMbs, urea denaturation curves were generated at pH 7.60 (Figure 4). This pH was chosen to ensure that the Asp-110 side chain of C110D was charged. The curves are reversible and independent of protein concentration over a 5-fold range.

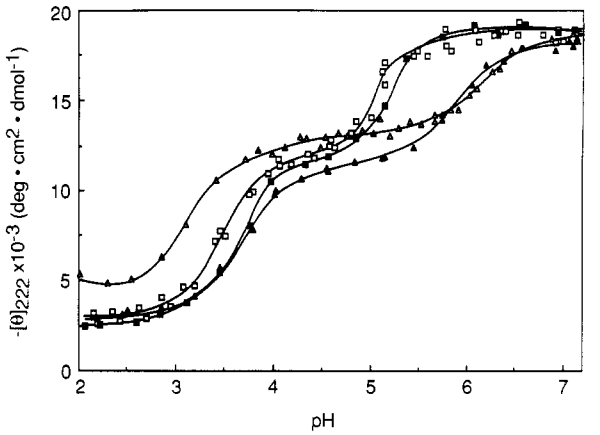

FIGURE 3: Acid denaturation of mutant human apoMbs. $[\theta]_{222}$ is plotted as a function of pH for C110A (□), C110S (■), C110D (▲), and C110L (△). Conditions were the same as in Figure 2 except that no dithiothreitol was added. Lines through the data points were drawn by inspection.

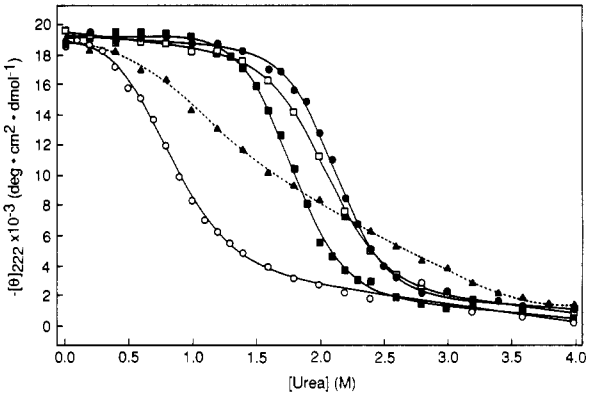

FIGURE 4: Urea denaturation of human apoMbs. $[\theta]_{222}$ is plotted as a function of urea concentration for wild-type (□), C110A (●), C110S (■), C110D (○), and C110L (▲). Solid lines are derived by nonlinear least-squares fitting to a two-state transition as described under Experimental Procedures except for C110L, for which the fitting program did not converge. The dashed line was drawn by inspection. Samples were measured at 3 °C and contained, in addition to urea, 1.00 μM apoMb and 10 mM HEPES, pH 7.60.

Except for C110L, the curves can be subjected to thermodynamic analysis by assuming that the folding/unfolding transition is two-state. As detailed under Experimental Procedures, the net free energy stabilizing the folded state in the absence of denaturant is estimated by linear extrapolation of ΔG_{app} values calculated in the transition region (Table II). $\Delta\Delta G°_{app}$ is the change in $\Delta G°_{app}$ caused by a given mutation, using wild-type as the basis for comparison. C110S and wild-type are essentially indistinguishable, while C110D, which places a charged residue in the helix packing site, is strongly destabilizing compared to wild-type ($\Delta\Delta G°_{app}$ = −3.6 ± 0.4 kcal/mol). C110A apoMb, on the other hand, is actually more

Table II: Denaturation Curve Analysis at pH 7.6[a]

	apomyoglobin[b]			holomyoglobin[c]		
protein	C_{mid}[d]	$\Delta G°_{app}$[e]	$\Delta\Delta G°_{app}$[f]	C_{mid}[d]	$\Delta G°_{app}$[e]	$\Delta\Delta G°_{app}$[f]
wild-type	2.05 (0.01)	5.1 (0.2)		1.40 (0.01)	7.8 (0.5)	
C110A	2.12 (0.01)	6.1 (0.3)	1.0 (0.4)	1.60 (0.01)	10.6 (0.5)	2.8 (0.7)
C110S	1.76 (0.01)	4.9 (0.3)	−0.2 (0.4)	1.43 (0.01)	8.3 (0.5)	0.5 (0.7)
C110D	0.70 (0.09)	1.5 (0.3)	−3.6 (0.4)	1.09 (0.01)	8.2 (0.5)	0.4 (0.7)
C110L	ND[g]	ND	ND	1.20 (0.01)	6.0 (0.5)	−1.8 (0.7)

[a] Standard deviations resulting from nonlinear least-squares analysis are given in parentheses. [b] Apomyoglobin parameters calculated from data in Figure 4 (urea denaturation at 3 °C). [c] Metmyoglobin parameters calculated from data in Figure 5 (GuHCl denaturation at 25 °C). [d] C_{mid} is the midpoint denaturant concentration given in molarity units. [e] $\Delta G°_{app}$ is given in kilocalories per mole. [f] $\Delta\Delta G°_{app}$ is the apparent free energy change in kilocalories per mole relative to the wild-type protein. [g] ND, not determined.

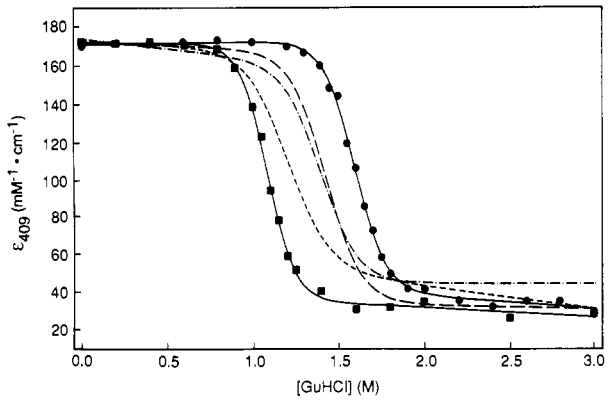

FIGURE 5: GuHCl denaturation of human Mbs (heme present). The extinction coefficient at 409 nm is plotted as a function of GuHCl concentration for wild-type (-·-), C110A (●), C110S (--), C110D (■), and C110L (---). Lines are derived by nonlinear least-squares fitting as described under Experimental Procedures. For clarity, actual data points are shown only for C110A and C110D; however, the fit is equally good for the remaining curves. Samples were measured at 25 °C and contained, in addition to GuHCl, 1 μM metMb and 10 mM HEPES, pH 7.60.

stable than the wild-type protein by 1.0 ± 0.4 kcal/mol.

Native C110L begins to unfold at a relatively low urea concentration, consistent with significant destabilization of the native state. The nonsigmoidal shape of its urea denaturation curve suggests, however, that the two-state assumption may break down for this mutant, implying that at least one equilibrium intermediate is present in the transition zone. Acid denaturation curves, discussed above, suggest that C110L is the least stable apoMb studied. The appearance of at least one intermediate in the urea denaturation of C110L thus supports the idea that destabilizing the native state can reveal equilibrium intermediates (see Discussion). Whether the intermediates observed in acid and urea denaturation are structurally related is not yet known.

The structures of several Mbs are known to high resolution. If the structures of apo- and holoproteins are similar, the impact of helix pairing site mutations on the stabilities of the apo- and holoproteins may also be similar. To examine the effect of helix pairing site mutations on the stability of the holoprotein, the Soret absorbance at 409 nm was monitored as a function of GuHCl concentration (Figure 5). $\Delta G°_{app}$ and $\Delta\Delta G°_{app}$ (Table II) are calculated as before from analysis of these transition curves. With one exception, C110D, the results are qualitatively similar to those obtained with the corresponding apoproteins. C110A is stabilizing relative to wild-type, C110S has little effect, and C110L, as expected, is destabilizing. Unlike C110L apoprotein, C110L holoprotein appears to unfold in a two-state transition. Because heme stabilizes the native holoprotein, the mutation C110L is probably insufficiently destabilizing to reveal intermediates. Surprisingly, though, C110D and wild-type Mbs have similar stabilities [$\Delta\Delta G°_{app}$ = 0.4 ± 0.7 kcal/mol]. In this case, compensating changes in the transition midpoint (C_{mid}) and the cooperativity (m) result in a similar free energy of unfolding, since $\Delta G°_{app} = RTmC_{mid}$ (Experimental Procedures).

Monitoring $[\theta]_{222}$ instead of ϵ_{409} yielded results which were identical within experimental error except in the case of C110A, for which $\Delta G°_{app}$ was 8.8 ± 0.6 kcal/mol (data not shown). The reason for this discrepancy is unknown.

Discussion

Intermediates in the Folding Reactions of Small Proteins. A fundamental hurdle in understanding protein folding is the difficulty of studying folding intermediates. Intermediates are much less stable under most conditions than the native and/or unfolded protein. Small single-domain proteins, seemingly the best model systems for attacking the folding problem, seldom exhibit measurable populations of intermediates at equilibrium, even in the denaturation transition zone between native and unfolded protein. Indeed, calorimetric studies of several small proteins show that unfolding is very close to a two-state transition, although the presence of small populations (<5%) of intermediates cannot be excluded (Privalov, 1979). Intensive efforts have therefore been directed at characterizing transient kinetic intermediates, either by covalently trapping them for further study (Creighton, 1984) or, more recently, by using a combination of rapid mixing techniques and two-dimensional ^{1}H NMR (Roder et al., 1988; Udgaonkar & Baldwin, 1988). Oas and Kim (1988) have developed a peptide model system for pancreatic trypsin inhibitor folding intermediates. Another approach, taken here, is to try to increase the equilibrium population of intermediate states in the transition zone to a level amenable to direct characterization.

Robson and Pain (1976) have suggested that an intermediate is observed in the guanidine hydrochloride (GuHCl)-induced denaturation reaction of penicillinase, but not for most other globular proteins, because native penicillinase is unusually unstable. According to this line of reasoning, denaturant concentrations (or temperatures) sufficient to denature most globular proteins severely destabilize equilibrium intermediates as well (Tanford, 1970; Robson & Pain, 1976). Generalizing from the penicillinase example, one might, by selectively destabilizing the native state of a protein, create a window in which the native state is unstable but intermediates are populated. For example, an equilibrium intermediate is observed for the unfolding of bovine α-lactalbumin only when Ca^{2+}, which stabilizes the native protein, is absent (Ikeguchi et al., 1986a). In this work, low temperature and site-directed mutagenesis have been used to destabilize the native state of human apoMb relative to one or more equilibrium intermediates. Acid denaturation of wild-type and mutant apoMbs shows directly that this is possible. The success of this attempt is also demonstrated by one mutant (C110L) for which urea denaturation is no longer two-state; i.e., stable intermediates are detected in the unfolding transition zone.

Helix–Helix Pairing. Mutations were chosen to disrupt, to varying degrees, interactions between the B and G helices of apoMb. We expected this helix pairing site to play a critical role in stabilizing the native state. Helix pairing is an important motif in known protein structures. Chothia et al. (1981) established that helix pairing usually entails the intercalation of ridges and grooves along the interacting helix faces. The most prominent ridges are formed by side chains at positions i, $i + 4$, $i + 8$, ..., etc. along an α-helix, since this spacing most closely corresponds to the helical repeat unit of 3.6 residues/turn. Intercalation of $\pm 4n$ ridges of one helix into $\pm 4n$ ridges of another helix defines an interhelical angle of about −50°, which is in fact seen in half of the helix pairings studied. The angle between B and G helices in sperm whale Mb is −55°; $\pm 4n$ ridges on the B helix intercalate among $\pm 4n$ ridges on the G helix (Lesk & Chothia, 1980). An elegant feature of the analysis by Chothia and co-workers is that, to this point, it is derived exclusively from the backbone geometry of the α-helix and consequently is independent of the specific amino acid sequence. The nature of the side chains, of course, plays an important role in determining the precise positioning of a helix–helix interaction (Lesk & Chothia, 1980; Chothia et al., 1981).

It seems reasonable that helix pairs are stabilized primarily by the burial of closely packed, hydrophobic side chains (Richmond & Richards, 1978), although hydrogen bonds and salt bridges between interacting helices, usually involving nonburied atoms, also occur quite often (Chothia et al., 1981). Mutations or modifications which disturb either the close packing or the hydrophobicity of a helix pairing site would then destabilize that interaction and consequently the protein. Several experiments indicate that helix pairing sites are indeed sensitive to these two types of disruption. Radding (1987) has chemically modified the two Trp residues of sperm whale Mb, which are located in the A·E and A·H helix pairing sites, to the less hydrophobic oxindolylalanine and has shown that this comparatively subtle change severely destabilizes the holoprotein. He also suggests that the acid denaturation of the modified Mb is no longer two-state. Alber and co-workers have isolated an Ala → Val mutation in a helix pairing site of bacteriophage T4 lysozyme which lowers protein stability by 4 kcal/mol, presumably as a result of steric clash involving the two additional methyl groups. Although the mutant lysozyme is active, the X-ray crystal structure shows that the helices are pried apart (T. Alber, personal communication). Low tolerance for mutations has been demonstrated recently for several residues buried in a helix pairing site between λ repressor monomers (Reidhaar-Olson & Sauer, 1988).

Stability of Native ApoMbs. In this study, single amino acid replacements of a cysteine residue buried in the G·B packing interface are shown to alter apoMb stability greatly. In particular, while the mutation C110S has little effect, C110D, which places a charged residue in the helix pairing site, is severely destabilizing. Comparing free energies of unfolding for C110D and wild-type apoMbs at pH 7.6, where Asp-110 is charged, $\Delta\Delta G°_{app}$ determined by urea denaturation is −3.6 ± 0.4 kcal/mol (Table II). C110L, which substitutes the much larger leucine residue for cysteine in the pairing site, also appears to destabilize native apoMb drastically: although the stability of the acid intermediate, I, is hardly affected, the N ↔ I transition midpoint is shifted +0.9 pH unit (Table I). C110A, in which a larger residue is replaced by a smaller one of comparable hydrophobicity, is *more* stable than wild-type (see below).

The destabilizing effect of C110D, and the (inverse) correlation between residue size and protein stability for the remaining four apoMbs, strongly suggests that both charged residues and residues which interfere with close packing can destabilize the G·B helix pairing site and consequently the protein. Both conclusions have been drawn for buried residues in other proteins: mutations which alter residue size or introduce polar or charged residues in place of more hydrophobic residues are generally more deleterious for protein stability at buried than at surface positions (Argos et al., 1979; Fermi & Perutz, 1981; Pakula et al., 1986; Alber et al., 1987).

Stability of HoloMbs. The stability of the corresponding holoMbs was assessed by GuHCl denaturation. The results are subject to some uncertainty (in addition to the standard deviations quoted in Table II which derive from the fitting routine) because the reversibility of the unfolding reaction was only 85–90%. In general, however, the effect of residue 110 replacements on Mb stability is similar to their effect on apoMb stability. This result adds to earlier evidence [see Griko et al. (1988) and references cited therein] that apoMb has a well-organized tertiary structure that is closely related to the structure of Mb. Compared to wild-type, C110S is similar in stability, while, as expected, C110L holoprotein is less stable ($\Delta\Delta G°_{app}$ = −1.8 ± 0.7 kcal/mol). As in the case of the apoproteins, C110A holoprotein is more stable than wild-type. Here, the difference in stability between wild-type and C110A is greater: $\Delta\Delta G°_{app}$ is 2.8 ± 0.7 kcal/mol for the holoprotein as opposed to 1.0 ± 0.4 kcal/mol for the apoprotein (Table II). If the presence of the heme group creates a less flexible protein interior, the effect of making a favorable change (Cys → Ala) may be magnified.

A surprising result is obtained for C110D holoprotein, which is approximately as stable as wild-type when judged by $\Delta G°_{app}$; when judged by the GuHCl concentration required to reach half-denaturation (C_{mid}), the C110D mutation is, however, strongly destabilizing. For apoMb, the C110D mutant is 3.6 kcal/mol less stable than wild-type.

The result that C110A is more stable than wild-type for both apo- and holoMbs is unexpected. In view of the recent study by Fersht and co-workers of the destabilizing effects of making small deletions in the hydrophobic core of barnase (Kellis et al., 1988), it is interesting to observe that the stability of Mb can be *increased* by making a small deletion in the hydrophobic core (C110A). Because cysteine is somewhat more hydrophobic than alanine (Cantor & Schimmel, 1980), this stability increase cannot be caused by an increase in the hydrophobicity of the packing site. It may be that the removal of the −SH group allows structural rearrangement which yields a more stable protein. Alternatively, the mutation C110A may relieve steric clash involving the −SH group without causing significant structural change. To distinguish these possibilities, and to understand better to what extent close packing of hydrophobic side chains stabilizes protein structure, high-resolution structures of these proteins are needed.

Stability of Acid Intermediates. ApoMb also provides an opportunity to study the effect of destabilizing the G·B helix–helix interaction on the stability of the compact acid intermediate. According to Ptitsyn (1987), the molten globule state (of which the acid intermediate of apoMb may be an example) is characterized by the absence of fixed side chain conformations. Presumably, helix pairing at the G·B site would require that side chains become fixed in this interaction. Acid denaturation of these apoMbs demonstrates that both the N ↔ I and I ↔ U transition midpoints change as the residue at position 110 is varied; these midpoint shifts clearly fail, however, to track each other with respect to a given mutant (see Table I). Whereas disruption of the G·B helix–helix interaction can account for the shifts in the N ↔ I transition, a different explanation is needed for the shifts in the I ↔ U transition.

Judged by the pH midpoint of the I ↔ U transition, the stability of the intermediates in relation to the unfolded proteins correlates very well with the hydrophobicity of residue 110 as measured by the transfer free energy from ethanol to water (Tanford, 1962; Cantor & Schimmel, 1980). Hence, apoMbs with hydrophobic residues such as Leu and Cys both have very stable intermediates, although the N ↔ I transition midpoints for these two proteins differ by 0.9 pH unit. That hydrophobicity seems to be the dominant factor suggests position 110 is at least partially buried in the intermediate. Recent mutagenic studies on several other proteins have demonstrated a close correlation between the thermodynamic stability of the native state and the hydrophobicity of single, mostly buried, residues (Matsumura et al., 1988; Yutani et al., 1987). Side chain size, however, seems to play little or no role in determining the stability of the apoMb I state, arguing that the structure of the intermediate in the vicinity of residue 110 is somewhat looser than the structure of the native protein.

The pH midpoint of the N ↔ I transition for wild-type apoMb is 5.3, which implicates histidine side chain ionization in the partial unfolding reaction. One possibility is that one or more buried histidine residues, uncharged at neutral pH, disrupt critical hydrophobic interactions upon protonation. Of the nine histidine residues in human Mb, six are buried in the interior of the protein (side chain surface-accessible area < 20 Å^2, based on the sperm whale Mb structure; Lee & Richards, 1971). Three of these contact the heme group, one is in the F·H helix pairing site, and the remaining two, His-24 and His-119, are in the G·B helix pairing site (Lesk & Chothia, 1980). A plausible scenario is that the partial unfolding that occurs in the N → I transition involves disruption of the G·B helix pairing site caused by protonation of His-24 and/or His-119. A prediction of this model is that disruptive mutations in the G·B helix pairing site, while destabilizing the N state, would have substantially less effect on the stability of the I state. This is indeed the case: the range of pH midpoints for the I ↔ U transition is less than half that seen for the N ↔ I transition (Table I).

A Novel Urea Intermediate. While measuring the stability of the native apoMbs to urea denaturation, we found that the folding–unfolding transition of C110L is remarkably broad and does not appear to be two-state. Initial estimates for six parameters are required by the nonlinear least-squares analysis program used to fit the data in these studies; no estimates tested allowed the iterative program to converge. The data thus appear inconsistent with the two-state model used, in which free energy varies linearly with urea concentration.

In a study of temperature-sensitive mutants of staphylococcal nuclease, Shortle and Meeker (1986) found several mutants for which both urea and GuHCl unfolding transitions were significantly broader than for wild-type. In the most dramatic case, a triple mutant is shown to unfold with a cooperativity (defined as $m = d \ln K_{app}/d[\text{denaturant}]$) about half that of wild-type. Most striking, denaturation curves generated by using two different probes for the denaturation process, intrinsic fluorescence and CD, have very different midpoints and cooperativities. While Shortle and Meeker argue that their results are best explained by postulating changes in the accessible surface area of the denatured proteins within the context of a two-state model, it seems possible that intermediates are being detected, at least in the case of the triple mutant. In particular, the noncoincidence of denaturation curves observed with two different probes is strong evidence for one or more equilibrium intermediates. The very broad transition seen for $[\theta]_{222}$ as a function of [GuHCl] for the nuclease triple mutant is quite similar to that seen in our study for the urea denaturation of C110L apoMb.

Relation to a Protein Folding Model. We have chosen to study apoMb in hopes of developing a system in which the predictions of the framework model are explicit and can be tested directly. If, as seems plausible, the structures of Mb and apoMb are similar, then according to the framework model the local structures which form earliest in folding must be helices and/or loops. Moreover, the second stage of folding must involve exclusively helix–helix pairing: the architectural simplicity of apoMb is such that helix–helix interactions comprise essentially the sole type of tertiary interaction. By altering a central residue in a representative helix–helix packing site, we have begun to characterize the contribution of interhelix contacts to apoMb stability. Results presented here clearly demonstrate that such contacts stabilize the native protein. In this work, we have failed to find single-site mutations which strongly affect the stability of the compact intermediate. This may imply that the structure of the intermediate is not well-defined, as would be the case for a molten globule. Alternatively, the acid intermediate may have a different and/or more flexible structure in the region of the G·B helix pairing site but have a well-defined structure overall. If so, it may be possible to affect the stability of the compact acid intermediate by targeting mutations to other helix pairing sites.

In summary, the results presented here demonstrate that mutations in the G·B helix pairing site can destabilize the native state of apoMb and thus enhance our ability to detect and study equilibrium folding intermediates. It remains to characterize the structures of the two types of intermediates—those observed during acid denaturation and those observed during urea denaturation—in greater detail.

Acknowledgments

We are indebted to P. Privalov for communication of results prior to publication, to S. Boxer, R. Varadarajan, D. Lambright, K. Nagai, and M. Zuber for gifts of materials used in this study, and to V. Robbins and R. Sapolsky for help in preparing the figures. We owe a special debt of gratitude to R. Varadarajan, whose suggestions and discussion throughout this work have been invaluable. We also thank T. Baker, D. Barrick, J. Carey, R. Fairman, E. Gavis, S. Marqusee, and A. Robertson for helpful comments on the manuscript.

References

Alber, T., Dao-pin, S., Nye, J. A., Muchmore, D. C., & Matthews, B. W. (1987) *Biochemistry 26*, 3754–3758.

Argos, P., Rossmann, M. G., Grau, U. M., Zuber, H., Frank, G., & Tratschin, J. D. (1979) *Biochemistry 18*, 5698–5703.

Balestrieri, C., Colonna, G., Giovane, A., Irace, G., & Servillo, L. (1976) *FEBS Lett. 66*, 60–64.

Cantor, C. R., & Schimmel, P. R. (1980) *Biophysical Chemistry*, p 52, Freeman, San Francisco.

Chothia, C., Levitt, M., & Richardson, D. (1981) *J. Mol. Biol. 145*, 215–250.

Cohen, F. E., Richmond, T. J., & Richards, F. M. (1979) *J. Mol. Biol. 132*, 275–288.

Colonna, G., Balestrieri, C., Bismuto, E., Servillo, L., & Irace, G. (1982) *Biochemistry 21*, 212–215.

Creighton, T. E. (1984) *Adv. Biophys. 18*, 1–20.

Dolgikh, D. A., Abaturov, L. V., Bolotina, I. A., Brazhnikov, E. V., Bychkova, V. E., Bushuev, V. N., Gilmanshin, R. I., Lebedev, Y. O., Semisotnov, G. V., Tiktopulo, E. I., & Ptitsyn, O. B. (1985) *Eur. Biophys. J. 13*, 109–121.

Edelhoch, H. (1967) *Biochemistry 6*, 1948–1954.

Fermi, G., & Perutz, M. F. (1981) *Haemoglobin and Myoglobin*, pp 97–101, Clarendon, Oxford.

Griko, Y. V., Privalov, P. L., Venyaminov, S. Y., & Kutyshenko, V. P. (1988) *J. Mol. Biol. 202*, 127–138.

Harrison, S. C., & Blout, E. R. (1965) *J. Biol. Chem. 240*, 299–303.

Ikeguchi, M., Kuwajima, K., & Sugai, S. (1986a) *J. Biochem. (Tokyo) 99*, 1191–1201.

Ikeguchi, M., Kuwajima, K., Mitani, M., & Sugai, S. (1986b) *Biochemistry 25*, 6965–6972.

Irace, G., Balestrieri, C., Parlato, G., Servillo, L., & Colonna, G. (1981) *Biochemistry 20*, 792–799.

Irace, G., Bismuto, E., Savy, F., & Colonna, G. (1986) *Arch. Biochem. Biophys. 244*, 459–469.

Kellis, J. T., Jr., Nyberg, K., Sali, D., & Fersht, A. R. (1988) *Nature (London) 333*, 784–786.

Kunkel, T. A., Roberts, J. D., & Zakour, R. A. (1987) *Methods Enzymol. 154*, 367–382.

Kuwajima, K., Nitta, K., Yoneyama, M., & Sugai, S. (1976) *J. Mol. Biol. 106*, 359-373.
Lee, G., & Richards, F. M. (1971) *J. Mol. Biol. 55*, 379-400.
Lesk, A. M., & Chothia, C. (1980) *J. Mol. Biol. 136*, 225-270.
Matsumura, M., Becktel, W. J., & Matthews, B. W. (1988) *Nature (London) 334*, 406-410.
Nagai, K., & Thogersen, H. C. (1984) *Nature (London) 309*, 810-812.
Oas, T. G., & Kim, P. S. (1988) *Nature (London) 336*, 42-48.
Ohgushi, M., & Wada, A. (1983) *FEBS Lett. 164*, 21-24.
Pace, C. N. (1986) *Methods Enzymol. 131*, 266-280.
Pakula, A. A., Young, V. B., & Sauer, R. T. (1986) *Proc. Natl. Acad. Sci. U.S.A. 83*, 8829-8833.
Privalov, P. L. (1979) *Adv. Protein Chem. 33*, 167-241.
Ptitsyn, O. B. (1987) *J. Protein Chem. 6*, 273-293.
Ptitsyn, O. B., & Rashin, A. A. (1975) *Biophys. Chem. 3*, 1-20.
Puett, D. (1973) *J. Biol. Chem. 248*, 4623-4634.
Radding, J. A. (1987) *Biochemistry 26*, 3530-3536.
Reidhaar-Olson, J. F., & Sauer, R. T. (1988) *Science 241*, 53-57.
Richmond, T. J., & Richards, F. M. (1978) *J. Mol. Biol. 119*, 537-555.
Robson, B., & Pain, R. H. (1976) *Biochem. J. 155*, 331-344.
Roder, H., Elove, G. A., & Englander, S. W. (1988) *Nature (London) 335*, 700-704.
Sanger, F. (1981) *Science 214*, 1205-1210.
Santoro, M. M., & Bolen, D. W. (1988) *Biochemistry 27*, 8063-8068.
Schellman, J. A. (1978) *Biopolymers 17*, 1305-1322.
Schellman, J. A. (1987) *Biopolymers 26*, 549-559.
Shortle, D., & Meeker, A. K. (1986) *Proteins: Struc., Funct., Genet. 1*, 81-89.
Takano, T. (1977) *J. Mol. Biol. 110*, 537-568.
Tanford, C. (1962) *J. Am. Chem. Soc. 84*, 4240-4247.
Tanford, C. (1970) *Adv. Protein Chem. 24*, 1-95.
Teale, F. W. J. (1959) *Biochim. Biophys. Acta 35*, 543.
Udgaonkar, J. B., & Baldwin, R. L. (1988) *Nature (London) 335*, 694-699.
Varadarajan, R. (1988) Ph.D. Thesis, Stanford University.
Varadarajan, R., Szabo, A., & Boxer, S. G. (1985) *Proc. Natl. Acad. Sci. U.S.A. 82*, 5681-5684.
Varadarajan, R., Lambright, D. G., & Boxer, S. G. (1989) *Biochemistry 28*, 3771-3781.
Yutani, K., Ogasahara, K., Tsujita, T., & Sugino, Y. (1987) *Proc. Natl. Acad. Sci. U.S.A. 84*, 4441-4444.

Flash Photolysis of the Serum Albumin–Heme–CO Complex†

M. C. Marden,*,‡ E. S. Hazard,§,‖ L. Leclerc,‡ and Q. H. Gibson‖

INSERM U299, Hôpital de Bicêtre, 94275 Le Kremlin Bicêtre, France, and Department of Biochemistry, Cellular and Molecular Biology, Cornell University, Ithaca, New York 14853

Received August 30, 1988; Revised Manuscript Received February 1, 1989

ABSTRACT: Protoheme–CO in aqueous solution does not exhibit a geminate ligand recombination reaction. Addition of a protein, either globin or serum albumin, to which heme binds strongly, leads to an observable geminate reaction in aqueous solution. The bimolecular kinetic data for the albumin–heme–CO complex show two stable components, one heme-like in rate and difference spectrum, and one hemoglobin-like. The geminate reaction correlates spectrally with the hemoglobin-like component.

The binding of heme to globins produces a holoprotein with remarkable properties including in the case of hemoglobin (Hb) the capacity to bind a number of gaseous ligands reversibly and cooperatively (Antonini & Brunori, 1971; Dickerson & Geis, 1983). The effect of the interaction of heme with globin can be seen clearly when the kinetics of the reactions of heme with carbon monoxide (CO) are compared with the corresponding reactions of hemoglobin (Marden et al., 1986). Binding to globin both protects the iron from oxidation and slows the entrance and exit of gaseous ligands from the heme pocket so that the ligands remain correlated with the heme long enough to allow appreciable recombination of the geminate pairs.

Globins, however, are not unique in binding to and modifying the behavior of heme. The protein hemopexin, for example, which is present in plasma, binds free heme in both ferro and ferri forms, and the ferro complex binds oxygen and CO reversibly (Muller-Eberhard & Morgan, 1975). Serum albumin is an abundant constituent of human plasma and has one high-affinity binding site with a dissociation constant of approximately 2×10^{-8} M for hemin as well as additional sites of much lower affinity (Adams & Berman, 1980; Beaven et al., 1974; Moehring et al., 1983).

The static spectrum of heme–albumin is intermediate between that of free heme and that of Hb. In methemalbumin the spectrum suggests that the iron is high spin, and this in turn implies that it may be bound to the protein through one of the many histidines in albumin (Kaminsky et al., 1972). Such axial ligand binding would be analogous both to Hb and to the hemopexin complexes (Brown, 1976; Muller-Eberhard & Morgan, 1975).

The analogy between heme binding to albumin and to globin suggested that an examination of ligand binding kinetics to the heme–albumin complex might help to show how important

† This work was supported in part by National Institutes of Health Grant GM-14276, National Science Foundation Grant 79-10446, and the Institut de la Santé et de la Recherche Médicale.

‡ INSERM.

§ Present address: Department of Cell and Molecular Pharmacology and Therapeutics, Medical University of South Carolina, Charleston, SC 29425.

‖ Cornell University.

0006-2960/89/0428-4422$01.50/0